

Multilayer ceramic composites with high failure resistance

Henryk Tomaszewski*, Helena Węglarz, Anna Wajler,
Marek Boniecki, Dariusz Kalinski

Institute of Electronic Materials Technology, Wolczynska 133, 01-919 Warsaw, Poland

Available online 19 May 2006

Abstract

Since Clegg et al. first fabricated SiC/C multilayer composites in 1990, multilayer ceramics have received much attention because of their improved properties achieved by designing weak interfaces. The weak interface can deflect the crack propagating perpendicularly to the plane of laminates repeatedly during fracture, thus leading to extremely high work-of-fracture. In this work multilayer composites of $\text{Al}_2\text{O}_3/\text{LaPO}_4$ were prepared using tape casting technique. Alumina slurry with acrylic latex binder was cast first on a polyester film, dried and then coated by LaPO_4 interlayer cast on it. The coated green tapes were dried, stacked and laminated. After the removal of the binder, the green body was hot pressed in argon atmosphere at 1280°C . A series of experiments were designed and conducted to investigate the influence of geometrical factors on mechanical properties of multilayer composites. Work-of-fracture of layered composites as high as 1100 J/m^2 has been found.

© 2006 Elsevier Ltd. All rights reserved.

Keywords: Layered ceramic composites

1. Introduction

Ceramics have many excellent properties that make their use as structural materials very attractive. However, their brittleness has prevented their use in structural application to date. The most promising candidates for improving ceramic brittleness have been continuous fiber ceramic composites, which have shown high strength and toughness.¹ These basic materials include silicon carbide or boron nitride layer between fiber and matrix, to weaken the fiber/matrix interface. Without a weak interface, the fiber-reinforced composites demonstrated catastrophic failure. However, the high fabrication cost of these materials and the high temperature oxidation of the interlayer and polymer-derived fibers remained a technological problems to solve. Ultimate materials occurred to be laminate composites,² where matrix and interlayer have been exchanged by oxides,^{3–5} behaving like carbon and boron nitride in non-oxide systems. A potential oxide interphase is lanthanum phosphate (LaPO_4), having a monazite structure, which was proposed by Morgan and Marshall⁶ and yttrium phosphate (YPO_4), with a xenotime structure evaluated by Kuo and Kriven.⁷

In this paper, all-oxide ceramics were fabricated by a low-cost, tape casting technique without incorporating expensive fibers. The material was LaPO_4 containing alumina laminate. A series of experiments were designed to investigate the influence of geometrical factors (thickness of matrix layer and interlayer) on crack propagation and mechanical properties of $\text{Al}_2\text{O}_3/\text{LaPO}_4$ multilayer ceramics.

2. Experimental procedure

Alumina (Taimicron TM-DAR from Taimei Chemicals Co., Japan) and LaPO_4 (Strem Chemicals Inc., USA) powders were used for fabricating multilayer composites by tape casting technique. The slurry formulation contained ~60 wt% oxide powder, ~30 wt% distilled water, ~10 wt% acrylic latex (DM765A, Clariant, Germany) as a binder and plasticizer and ~0.1 wt% dispersant (Dispex A-40, Allied Colloids Co., Great Britain). Alumina slurry was cast first to yield laminae of 50–300 μm thickness, dried and then coated by LaPO_4 interlayer of 10–100 μm thickness cast on it. The double green tapes were dried, punched into a rectangle (40 mm \times 80 mm), stacked and laminated by uniaxial and isostatic cold pressing. After the removal of the organic additives, the green body was hot pressed in argon atmosphere at 1280°C . The hot pressed samples were cut and ground to the dimensions of 45 mm \times 4 mm \times 4 mm or 45 mm \times 4 mm \times 2 mm.

* Corresponding author. Tel.: +48 22 8353041x472; fax: +48 22 834 9003.
E-mail address: henryk.tomaszewski@itme.edu.pl (H. Tomaszewski).

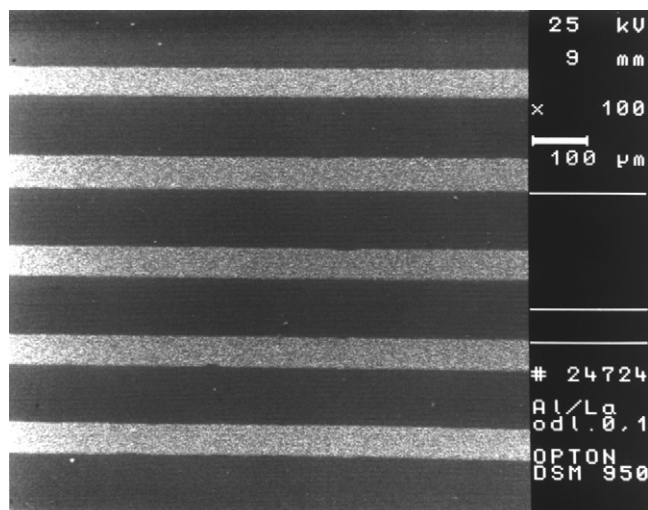


Fig. 1. Typical micrograph showing polished surface of layered composite: Al_2O_3 layer (dark one) and LaPO_4 layer (light one) with thickness of 100 and 50 μm , respectively.

The microstructure of composites was observed by scanning electron microscope (SEM) of OPTON DSM 950. Typical micrograph is shown in Fig. 1.

The bending strength of composites was determined on square bars having the dimensions 45 mm \times 4 mm \times 4 mm perpendicularly to the layers in three-point bending tests using a universal testing machine (Model 1446, Zwick) with 1 mm/min loading speed and 35 mm bearing distance.

For measurement of Young's modulus the beams were thinned to the height of 1 mm and then the compliance of the samples was recorded during loading tests with 0.1 mm/min loading speed and 40 mm bearing distance. The values of Young's modulus were determined using the relationship given by Fett and Munz.⁸

The controlled crack growth tests were performed on notched bars with one surface perpendicular to the layers polished and dimensions 45 mm \times 4 mm \times 2 mm during three-point bending with 5 $\mu\text{m}/\text{min}$ loading speed and 40 mm bearing distance. The path of the crack during fracture was registered by optical microscope and SEM. All experiments were done at room temperature in normal air environments. Regarding that the area under the recorded load–deflection curve of the specimen is the sum of the work used for creating of two new surfaces and the elastic strain energy of the system and sample studied, the work-of-fracture, γ_F , was determined.⁵

In all cases 10 composite samples has been used to determine bending strength and work-of-fracture and calculate standard deviation.

3. Results

As can be seen from Figs. 2 and 3 component materials of $\text{Al}_2\text{O}_3/\text{LaPO}_4$ layered composite fracture catastrophically at loading speed used in controlled crack growth tests. Bending strength and work-of-fracture both of these materials are listed

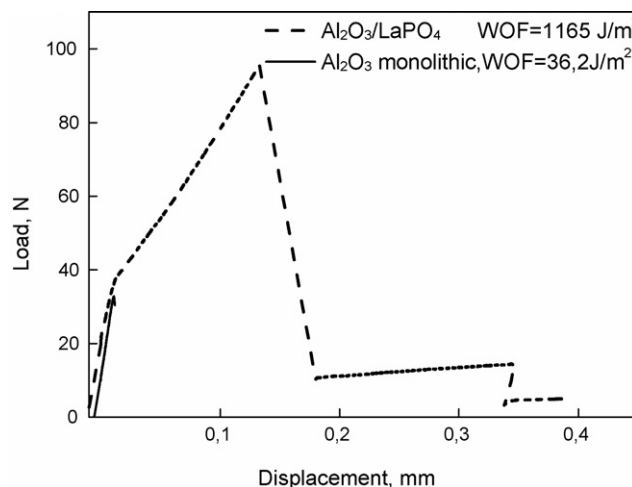


Fig. 2. Typical load–displacement curves of $\text{Al}_2\text{O}_3/\text{LaPO}_4$ multilayer composite (matrix layer of 100 μm and LaPO_4 of 20 μm) and monolithic Al_2O_3 prepared at the same conditions.

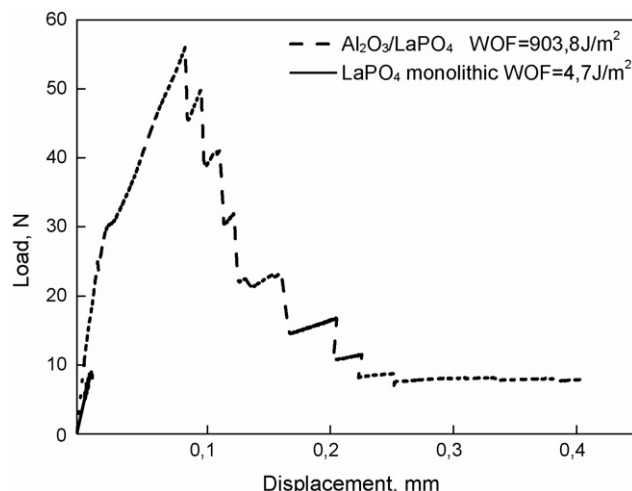


Fig. 3. Typical load–displacement curves of $\text{Al}_2\text{O}_3/\text{LaPO}_4$ multilayer composite (matrix layer of 200 μm and LaPO_4 of 20 μm) and monolithic LaPO_4 prepared at the same conditions.

in Table 1. The load–displacement responses of multilayer composites, shown in Figs. 2 and 3, are characteristic of the non-catastrophic fracture. To reveal the detailed nature of the fracture, the flexural test of the laminates for some samples was stopped before the bend bar broke and the specimens were examined under optical and scanning electron microscopes. As it occurred, the first slope change in the elastic region of the load–displacement curve seen at about 35–40 N load can be

Table 1

Comparison of mechanical properties of monolithic component materials and $\text{Al}_2\text{O}_3/\text{LaPO}_4$ multilayer composite

Material	Bending strength (MPa)	Work-of-fracture (J/m^2)
Al_2O_3	432.3 ± 10.2	36.2 ± 3.2
LaPO_4	103.0 ± 5.2	4.7 ± 0.5
$\text{Al}_2\text{O}_3/\text{LaPO}_4$ composite	356.3 ± 25.6	1165.1 ± 120.1

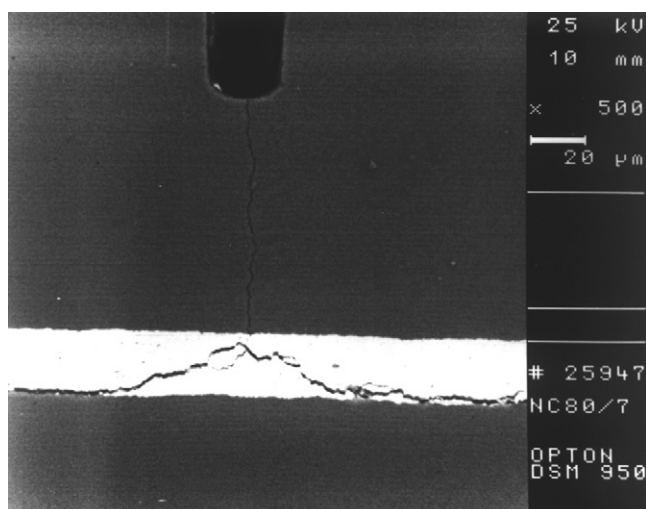


Fig. 4. Path of the crack propagating through layered composite for loading stopped at 50 N (just after the first slope change in the elastic region of the load–displacement curve shown in Fig. 2).

related to cracking of the matrix layer (Fig. 4). After opening at the bottom of the notch crack propagates through the matrix layer perpendicularly and then deflects in the LaPO_4 layer running at the interface to the left and right side. Continuous load increase is observed at the load–displacement curve during delamination. The delaminated interfaces extend laterally up to some millimetres to the outer loading points, but do not run to the end of the test bar. The laminate delaminates up to the first load drop and dissipates the strain energy by creating free surfaces. At this stage, the Al_2O_3 layer plays an important role. This strong layer supports the applied load, which keeps the delaminated composite from fracturing catastrophically. At the first load drop accumulated strain energy occurs to big and crack propagates perpendicularly, running through some pairs of alumina/lanthanum phosphate layers. Close relation between volume of the first load drop, thickness of the matrix layer and amount of matrix layer broken was observed. In the case of matrix layers 100 μm thick crack crossed 8–11 pairs of layers (see Fig. 5). Amount of layers crossed is dependent on the volume of load at the first load drop and varies from sample tested to sample influencing the final value of work-of-fracture. For thicker matrix layers the first drop of the load appears at lower load and only two of the matrix composite layers break (see Figs. 3 and 6), which can be related to lower amount of accumulated strain energy. After the first load drop, crack stops at matrix/interlayer interface, then propagates parallel to the layers leading to the following load extend at the load–displacement curve. At the second load drop only two pairs of layers break independent of matrix layer thickness (see Figs. 6 and 7). As the cracking/delamination events continue, the load–displacement curve looks like saw teeth and a non-brittle fracture response is achieved. This fracture behaviour is similar to that occurring in fiber-reinforced ceramic composites having a weak interface. Interfacial debonding and delamination are followed by load redistribution among unfractured part and the unbroken fibers. Interfacial delamination as seen in this study is an important toughening mechanism operat-

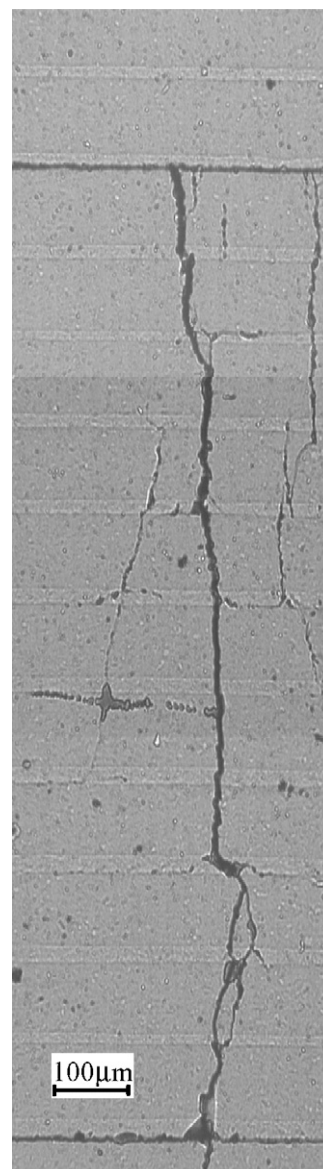


Fig. 5. Optical micrograph showing the crack path after the first load drop from the load–displacement curve presented in Fig. 2.

ing in flaw-tolerant ceramics, more effective than those of crack deflection, crack branching and microcracking, which operate in most particulate and laminated composites with strong interfaces.⁵

As shown in Table 1, $\text{Al}_2\text{O}_3/\text{LaPO}_4$ layered composites demonstrate good mechanical properties. As compared with monolithic alumina, this oxide laminate has a comparable mechanical strength, but excellent work-of-fracture. To find the influence of geometrical factors (thickness of matrix layer and interlayer) on crack propagation and mechanical properties of $\text{Al}_2\text{O}_3/\text{LaPO}_4$ multilayer ceramics two series of laminates with matrix layer thickness or interlayer thickness constant were prepared. As it was observed, delaminating crack always runs at matrix/interlayer interface independent of interlayer thickness (Fig. 8). It means that decrease of interlayer thickness keeping Al_2O_3 layer thickness constant can lead to increase of matrix layer/interlayer pairs amount in composite sample and

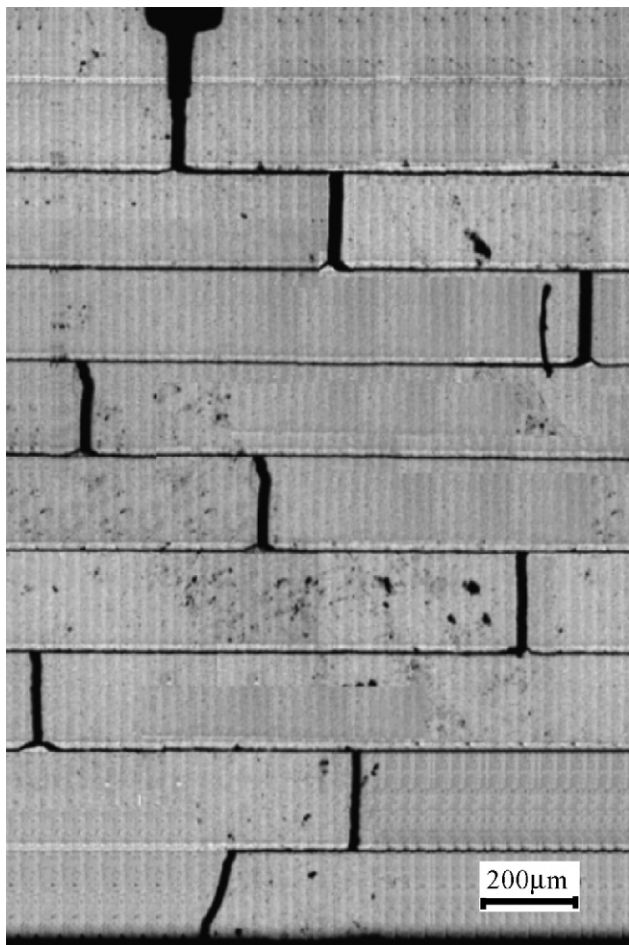


Fig. 6. Optical micrograph showing the crack path responsible for load–displacement curve shown in Fig. 3.

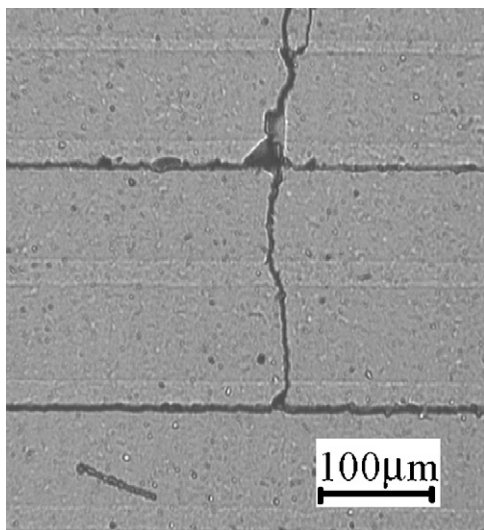


Fig. 7. Optical micrograph showing the crack path after the second load drop from the load–displacement curve presented in Fig. 2.

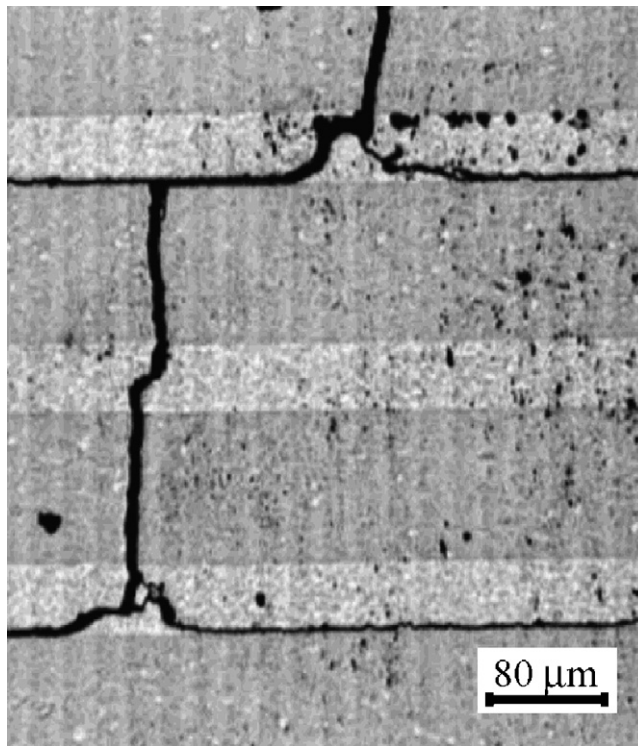


Fig. 8. Optical micrograph showing the path of delaminating crack in $\text{Al}_2\text{O}_3/\text{LaPO}_4$ multilayer composite with 40 μm thick LaPO_4 interlayer.

amount of cracking/delamination events responsible for non-catastrophic fracture. According to this thesis work-of-fracture of $\text{Al}_2\text{O}_3/\text{LaPO}_4$ multilayer ceramics shown in Fig. 9 strongly increases with interlayer thickness decrease. Similar curve of bending strength versus interlayer thickness is investigated from Fig. 10. In multilayer ceramics, bending strength is mainly determined by matrix layers. Their amount increases with decreasing interlayer thickness resulting in a small but increase of composite strength.

Similar influence on composite work-of-fracture is observed (Fig. 11), when Al_2O_3 layer thickness decreases at interlayer

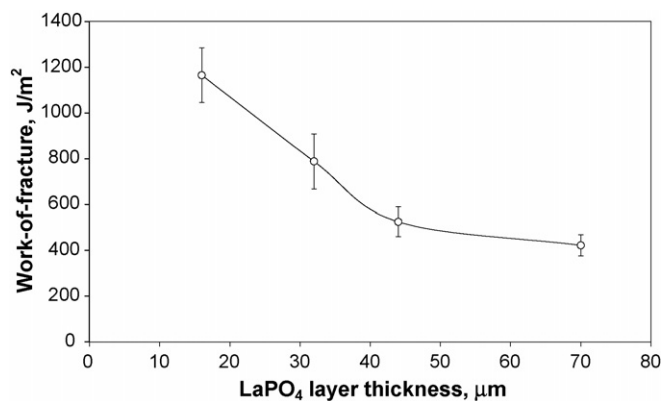


Fig. 9. Work-of-fracture as a function of LaPO_4 interlayer thickness for $\text{Al}_2\text{O}_3/\text{LaPO}_4$ multilayer composite with Al_2O_3 layer thickness (100 μm) constant.

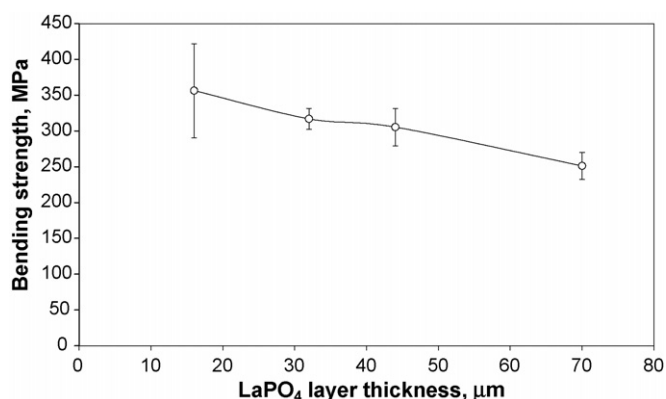


Fig. 10. Bending strength as a function of LaPO₄ interlayer thickness for Al₂O₃/LaPO₄ multilayer composite with Al₂O₃ layer thickness (100 μm) constant.

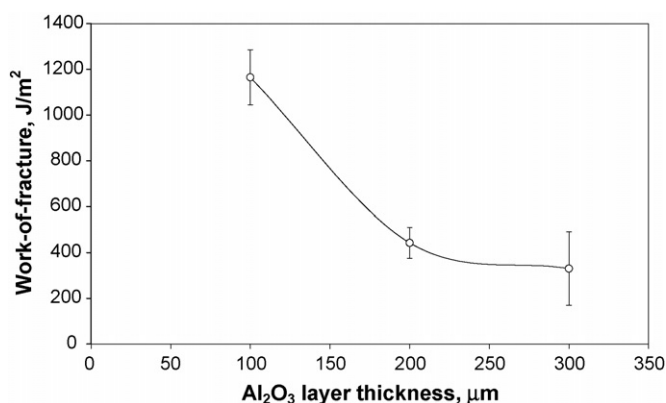


Fig. 11. Work-of-fracture as a function of Al₂O₃ matrix layer thickness for Al₂O₃/LaPO₄ multilayer composite with LaPO₄ interlayer thickness (20 μm) constant.

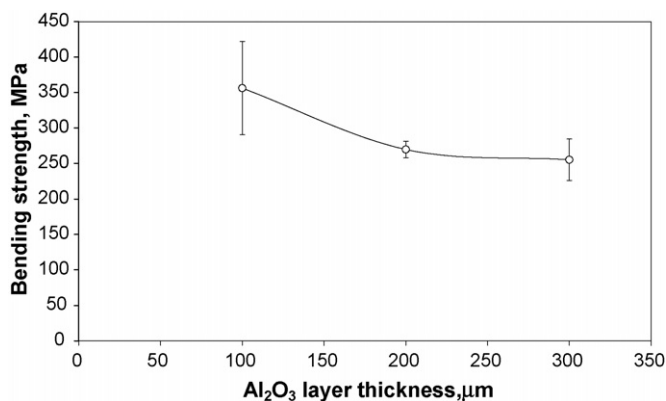


Fig. 12. Bending strength as a function of Al₂O₃ matrix layer thickness for Al₂O₃/LaPO₄ multilayer composite with LaPO₄ interlayer thickness (20 μm) constant.

thickness constant. Matrix layer thickness decrease increases the amount of cracking/delamination events that reflects in an increase of fracture energy adsorbed during fracture. According to Fig. 12 bending strength of laminate decreases when matrix layer thickness increases.

4. Conclusions

In this work LaPO₄ containing Al₂O₃ laminates with conventional two-layer configuration were fabricated and studied. Oxide laminate with high strength and work-of-fracture was obtained exhibiting extended interfacial delamination. The influence of geometrical factors (thickness of matrix layer and interlayer) on mechanical properties of Al₂O₃/LaPO₄ multilayer ceramics was found.

References

1. Evans, A. G., Perspective on the development of high-toughness ceramics. *J. Am. Ceram. Soc.*, 1990, **73**(2), 187–206.
2. Clegg, W. J., Kendall, K., Alford, N. McN., Button, J. D. and Birchall, J. D., A simple way to make tough ceramics. *Nature*, 1990, **347**, 455–457.
3. Marshall, D. B., Lange, F. F. and Ratto, J. J., Enhanced fracture toughness in layered microcomposites of Ce–ZrO₂ and Al₂O₃. *J. Am. Ceram. Soc.*, 1991, **74**(12), 2979–2987.
4. Marshall, D. B., Design of high-toughness laminar zirconia composites. *Ceram. Bull.*, 1992, **71**(6), 969–973.
5. Tomaszewski, H., Węglarz, H., Boniecki, M. and Rečko, W., Effect of barrier layer thickness and composition on fracture toughness of layered zirconia/alumina composites. *J. Mater. Sci.*, 2000, **35**(16), 4165–4176.
6. Morgan, P. E. D. and Marshall, D. B., Ceramic composites of monazite and alumina. *J. Am. Ceram. Soc.*, 1995, **78**(6), 1553–1563.
7. Kuo, D. H. and Kriven, W. M., Fracture of multilayer oxide composites. *Mater. Sci. Eng. A*, 1998, **241**, 241–250.
8. Fett, T. and Munz, D., Subcritical crack growth of macrocracks in alumina with R-curve behaviour. *J. Am. Ceram. Soc.*, 1992, **75**(4), 958–963.